JOURNAL OF BACTERIOLOGY, Feb. 2006, p. 1540–1550 Vol. 188, No. 4
0021-9193/06/$08.00+0 doi:10.1128/JB.188.4.1540–1550.2006

Influence of CrgA on Assembly of the Cell Division Protein FtsZ during Development of *Streptomyces coelicolor*

Ricardo Del Sol,[1] Jonathan G. L. Mullins,[1] Nina Grantcharova,[2] Klas Flärdh,[3] and Paul Dyson[1]*

Institute of Life Science, School of Medicine, University of Wales Swansea, Singleton Park, Swansea SA2 8PP, United Kingdom[1]; Department of Cell and Molecular Biology, Uppsala University, BMC, Box 596, SE-751 24 Uppsala, Sweden[2]; and Department of Cell and Organism Biology, Lund University, Sölvegatan 35, SE-223 62 Lund, Sweden[3]

Received 17 October 2005/Accepted 22 November 2005

The product of the *crgA* gene of *Streptomyces coelicolor* represents a novel family of small proteins. A single orthologous gene is located close to the origin of replication of all fully sequenced actinomycete genomes and borders a conserved gene cluster implicated in cell growth and division. In *S. coelicolor*, CrgA is important for coordinating growth and cell division in sporogenic hyphae. In this study, we demonstrate that CrgA is an integral membrane protein whose peak expression is coordinated with the onset of development of aerial hyphae. The protein localizes to discrete foci away from growing hyphal tips. Upon overexpression, CrgA localizes to apical syncytial cells of aerial hyphae and inhibits the formation of productive cytokinetic rings of the bacterial tubulin homolog FtsZ, leading to proteolytic turnover of this major cell division determinant. In the absence of known prokaryotic cell division inhibitors in actinomycetes, CrgA may have an important conserved function influencing Z-ring formation in these bacteria.

Studies of the model organism *Streptomyces coelicolor* have provided an informative framework with which to understand aspects of growth and regulation in the large number of species belonging to the genus and also in other actinomycetes. Reproductive growth in *Streptomyces* involves the formation of filamentous aerial hyphae that undergo differentiation into chains of unigenomic spores. Antibiotic production is often coincident with the onset of aerial growth. Several genes that are critical to various stages of this differentiation have been described in *S. coelicolor*, including *bld* genes, required for the initial growth of aerial hyphae, and *whi* genes, which are needed for the subsequent development of spore chains (4, 19). We previously characterized a novel developmental gene, *crgA*, which has a role in coordinating aspects of reproductive growth in *S. coelicolor* (6). Disruption of *crgA* results in precocious growth of aerial hyphae and early antibiotic production on glucose-containing solid media. Under these growth conditions, subsequent development of aerial hyphae was also affected in the mutant, resulting in the development of long chains of cells with an abnormal swollen morphology. This is consistent with a model in which CrgA normally acts to inhibit sporulation septation prior to growth arrest of aerial hyphae. Indeed, overexpression of the protein, uncoupling its carbon source and growth phase-dependent regulation, results in a Whi phenotype on any sporulation medium, with growth of aerial hyphae lacking sporulation septa. No effects on septation in vegetative hyphae have been observed in either *crgA* disruption or overexpression mutants.

The first recognizable step of bacterial cell division is the assembly of FtsZ into a ring-like structure (1, 8, 25). The Z ring is associated with the cytoplasmic membrane and drives cytokinesis. Z-ring formation is dependent on the balance between FtsZ polymerization and depolymerization (31, 35). This balance is influenced either by cell division inhibitors that prevent inappropriate Z-ring formation, such as MinC in *Escherichia coli* (17) and EzrA in *Bacillus subtilis* (14, 24), or by proteins that stabilize FtsZ polymers, such as ZipA in *E. coli* (30). A single *ftsZ* gene is required for two types of septation in *S. coelicolor*: infrequent cross wall formation that separates nondetached syncytial cells in the vegetative mycelium, and the multiple synchronous septation of the aerial hyphae that leads to the formation of unigenomic spores (34). These developmentally distinct types of cell division are in part a consequence of how the *ftsZ* gene is regulated: there are two promoters, one of which is specifically activated in the aerial hyphae (10). In addition, the isolation of a missense mutation in *ftsZ* that preferentially affected sporulation septation indicated that there are differences in Z-ring assembly between vegetative and sporogenic hyphae (13). For the latter, none of the systems that have been implicated in selection of division sites in other bacteria appear to have a role. Thus, while nucleoid occlusion affects the formation of Z rings in *E. coli* and vegetative cells of *B. subtilis* (15, 26), the early stages of sporulation septation in *Streptomyces* often occur over nonsegregated chromosomes, and separation of nucleoids is not observed until septal constriction has started (9, 34). The *S. coelicolor* genome lacks obvious homologs of known prokaryotic cell division inhibitors, such as MinC and EzrA.

Given the cytological observations of aberrant sporulation septation due to either a lack or overabundance of CrgA, we have investigated whether it can inhibit Z-ring formation in aerial hyphae of *S. coelicolor*. We report on the expression, topology, and localization of CrgA and explore how its expression affects the dynamic assembly of the FtsZ protein in vivo.

* Corresponding author. Mailing address: Institute of Life Science, School of Medicine, University of Wales Swansea, Singleton Park, Swansea SA2 8PP, United Kingdom. Phone: 44-1792 295667. Fax: 44-1792 295447. E-mail: p.j.dyson@swansea.ac.uk.

TABLE 1. Bacterial strains and plasmids

Strain or plasmid	Characteristics	Reference or source
Strains		
S. coelicolor M145	Prototrophic; SCP1$^-$ SCP2$^-$	16
S. coelicolor DC3845	M145 Δ*crgA*::*tsr*	6
E. coli JM109	F′ *traD36 proA*$^+$*B*$^+$ *lacI*^{q} Δ(*lacZ*)*M15*/Δ(*lac-proAB*) *glnV44* e14 *gyrA96 recA1 relA1 endA1 thi hsdR17*	40
E. coli ET12567(pUZ8002)	*dam13*::Tn*9 dcm-6 hsdM hsdR recF143 zjj-201*::Tn*10 galK2 galT22 ara14 lacY1 xyl-5 leuB6 thi-1 tonA31 rpsL136 hisG4 tsx-78 mtlI glnV44*, containing the nontransmissible *oriT* mobilizing plasmid pUZ8002	11
Plasmids		
pSET152	Integrative vector for *Streptomyces; oriT*(RK2) *int attP* (ΦC31) *aac*(*3*)*IV*	2
pIJ8600	Integrative *tipAp* expression vector for *Streptomyces; oriT*(RK2) *int attP* (ΦC31) *aac*(*3*)*IV*	36
pIJ8660	Integrative vector for *Streptomyces*, promoterless *eGFP, oriT*(RK2) *int attP* (ΦC31) *aac*(*3*)*IV*	36
pFP14	*eGFP* coding sequence flanked by several restriction sites, NdeI site at start codon; *bla*	P. Herron, unpublished data
pVC119	Promoterless *luxAB* operon from *Vibrio harveyi*, preceded by in-frame stop codons and ribosome-binding site, *kan*	P. Herron, unpublished data
pRLux86	Promoterless *luxAB* operon, flanked by transcription terminators, *aac*(*3*)*IV*	This study
pSC3854	*S. coelicolor crgA* in pSET152	6
pSC3854XbaI	pSC3854 with an XbaI site introduced at position corresponding to amino acid 22 in *crgA* coding sequence	This study
pSC3854m1	pSC3854, NdeI site at start codon of *crgA*	This study
pRIR1	*crgA* promoter transcriptionally fused to *luxAB*	This study
pET26b(+)	*kan*, T7 promoter, His-tag expression vector	Novagen
pME40	*crgA* coding sequence, NdeI at start codon	6
pRME45	pET26b(+) containing *crgA* coding sequence fused to His tag at C end	This study
pRWHis1	*crgA*::$[His]_6$ downstream of *ptipA*	This study
pRWHis2	*crgA*::$[His]_6$ downstream of native promoter	This study
pRME43	*crgA*::*eGFP* downstream of *ptipA*	This study
pHL219	pUWL219 (21) derivative, hygromycin^r	This study
pHLHis1	pHL219 derivative, P_{tipA}::*crgA*::his_6	This study
pKF41	*ftsZ*::*eGFP*	12

MATERIALS AND METHODS

Bacterial strains, growth conditions, and conjugal transfer from *E. coli* to *Streptomyces*. The bacterial strains used in this study are listed in Table 1. *Streptomyces* strains were cultured on NE (1% glucose, 0.2% yeast extract, 0.2% meat extract, 0.2% Casamino Acids, and 2% agar; pH 7), mannitol soy agar, or NMMP agar, omitting polyethylene glycol 6000 and supplemented with glucose (final concentration, 0.5%), as previously described (21). *Escherichia coli* ET12567 containing pUZ8002 was used for intergeneric conjugation of plasmids into *S. coelicolor* (32). pUZ8002 supplies transfer functions to *oriT*-containing plasmids but is not efficiently transferred itself because of a mutation in its own *oriT*.

Plasmid constructions. The plasmids used are listed in Table 1; mutagenesis oligonucleotides are listed in Table 2. General procedures for DNA manipulation were used (33). All DNA manipulations were carried out using *E. coli* JM109 as the host. Plasmid constructs were verified by DNA sequencing. Oligonucleotides used for PCR amplification, site-directed mutagenesis, and quantitative PCR (Q-PCR) are listed in Table 2. Beacon Design 2.0 software (Premier Biosoft) was used for oligonucleotide design.

(i) Transcriptional fusion to luciferase. Plasmid pIJ8660 was digested with NdeI/NotI to remove *eGFP* and ligated to an NdeI/EagI DNA band from pVC119 (containing the *luxAB* operon), generating pRLux86. Site-directed mutagenesis of pSC3854 was used to create an XbaI restriction site at the position corresponding to amino acid 22 of the *crgA* coding sequence (changing 5′-CCA GCATCAA to 5′-CCTCTAGAAA), generating plasmid pSC3854XbaI. This plasmid was digested with XbaI, and the DNA fragment containing the *crgA* upstream sequence and coding sequence for the first 22 amino acids was ligated to pRLux86 digested with XbaI, resulting in pRIR1, which contains the insert in the desired orientation, i.e., *crgA* transcriptionally fused to *luxAB*.

(ii) CrgA translational fusion to His_6. Plasmid pME40 (6) was used as a template for site-directed mutagenesis to create a BamHI site, replacing the *crgA* native stop codon (changing 5′-AAGTAGCCCC to 5′-AAGGATCCCC). The resulting plasmid, pRME40 was digested with NdeI/BamHI and ligated to pET26b(+) digested with NdeI/BamHI, generating pRME45. Plasmid pIJ8600 was digested with BamHI, blunt ended, and then digested with NdeI, followed by ligation to a NdeI/SmaI DNA fragment released from pRME45, containing *crgA*:$[His]_6$ and a 1-kb fragment from the vector pET26b(+), resulting in plasmid pRWHis1. In order to place *crgA*:$[His]_6$ under the control of the *crgA* native promoter, plasmid pSC3854 was mutagenized to introduce an NdeI site at the *crgA* start codon (changing 5′-CCCTCGTGCC to 5′-CCCATATGCC), resulting in pSC3854m1. Restriction of pSC3854m1 with XbaI/NdeI released a fragment containing the *crgA* upstream sequence, which was then ligated to both pSET152 digested with XbaI/EcoRV and to an NdeI/SmaI DNA fragment released from pRME45. The resulting plasmid was named pRWHis2. The P_{tipA}:*crgA*:$[His]_6$ cassette was excised from pRWHis1 using KpnI, and the DNA fragment was subcloned into pHL219 digested with KpnI, generating pHLHis.

(iii) CrgA translational fusion to *eGFP*. Plasmid pME40 was digested with NdeI/BamHI and ligated to pIJ8600 similarly digested, generating plasmid pRME42. The *eGFP* coding sequence was released from pFP14 as a BamHI fragment and ligated to pRME42 previously digested with BamHI/BglII, resulting in plasmid pRME43.

Luciferase activity detection. For solid medium, black 96-well microplates were used to grow the strains under study. A 300-μl volume of agar medium was added into each well. One to 2 μl from a spore suspension was pipetted onto the agar medium and incubated at 28°C for the desired period of time. Luciferase activity was detected by adding an exogenous substrate, *n*-decanal (Sigma), as a vapor. The substrate was added onto a filter paper, which was then laid on top of the plate with the lid of the plate placed on top. After 3 min of incubation at room temperature to allow the substrate to diffuse into the cells, the light emission was quantified with an Anthos Lucy 1 microplate luminometer, with 0.1-s integration. At least three independently grown cultures were assayed in this way, and a negative control, consisting of the strain under study carrying a plasmid, pRLux86, containing a promoterless *luxAB* operon, was used in triplicate as well. The luminometer counts measured for the negative control were ≤0.1 for each time point.

TABLE 2. Oligonucleotides used

Assay and site	Oligonucleotide name	Sequence
Site-directed mutagenesis[a]		
XbaI site at codon 22 on *crgA*	crgAXba1	5′ CGAAGCAGGCGACC**TCTAGA**AAGCTGACCAGC
	crgAXba2	5′ GCTGGTCAGCTT**TCTAGA**GGTCGCCTGCTTCG
BamHI site at *crgA* stop codon	CrgAend1	5′ CGACGCAGTGGAA**GGATCC**CCGGCGGTGG
	CrgAend2	5′ CCACCGCCGG**GGATCC**TTCCACTGCGTCG
NdeI site at *crgA* start codon	crgA1	5′ CGACAGGAGAGACC**CATATG**CCGAAGTCACG
	crgA2	5′ CGTGACTTCGG**CATATG**GGTCTCTCCTGTCG
PCR		
S1 probe[b]	S1CrgAS	5′ **GCGGGA**ATTCGGTGCCCTTCGCGGTATCG
	S1CrgAAS	5′ GCTGGTCGCCTGCTTCGAGG
Q-PCR target genes		
hrdB	hrdBFor	5′ CCTCCGCCTGGTGGTCTC
	hrdBRev	5′ CTTGTAGCCCTTGGTGTAGTCG
crgA	crgARTfor	5′ AGGCGACCAGCATCAAGC
	crgARTrev	5′ CCACCACGATGTTCCAGTTG
16S rRNA	rRNA16F	5′ GCAGGCTAGAGTTCGGTAG
	rRNA16R	5′ CTCCTCAGCGTCAGTATCG
ftsZ	ftsZRTF1	5′ GCAGCACCGCAGAACTAC
	ftsZRTR1	5′ AGACCGACCTCGATCATCC

[a] Restriction sites are in boldface.
[b] Nonhomologous tail is indicated in boldface.

RNA isolation and S1 protection assay. Total RNA was isolated from cultures grown on cellophane disks on the surface of agar plates, using QIAGEN RNeasy Midi kits. For each isolation, the total RNA concentration was determined spectrophotometrically and the quality of the isolated RNA was analyzed on a 1.5% denaturing Tris-acetate-EDTA–agarose–formaldehyde gel as described elsewhere (33). The S1 probe was amplified by PCR using pSC3854 as template, encompassing from 300 nucleotides upstream to 60 nucleotides downstream of the *crgA* translation start codon. The nonhomologous tail (3) included in the S1CrgAS primer (sense strand) permitted distinction between full-length protection and probe-probe reannealing. The amplified probe was purified from an agarose gel and labeled at both 5′ ends using [γ-^{32}P]ATP and T4 polynucleotide kinase (NEB), followed by cleaning with a QIAquick PCR purification kit (QIAGEN). *hrdB* was used as a control for the S1 protection assay, as described previously (32). S1 nuclease protection assays were performed as described previously (21). Briefly, 20 μg total RNA was dried in a vacuum centrifuge and hybridized to 100 to 200 cpm of γ-^{32}P-labeled probe in Na-trichloroacetic acid at 70°C for 10 min and then 45°C for 15 h. The reaction mixture was treated with S1 nuclease (100 units), precipitated with isopropanol, and resuspended into loading dye. Samples were then denatured and separated on a polyacrylamide-urea sequencing gel alongside a sequencing ladder generated using primer S1CrgAS.

Real-time Q-PCR. cDNAs were obtained from RNA purified as described above, using a RETROscript reverse transcription kit (Ambion) and random decamers. Real-time PCR were carried out on an iCycler iQ real-time PCR detection system (Bio-Rad). Briefly, 5 μl of cDNA was mixed with 10 μl of iQ SYBR Green supermix (ABgene) and 10 pmol of each primer in a 20-ml final volume. The mix was submitted to the following thermal cycles: 15 min at 95°C followed by 50 cycles of 15 s at 94°C, 30 s at 57°C, and 30 s at 72°C, continued with 30 s at 55°C, 30 s at 95°C, and 40 steps of 10 s with a temperature gradient increase of 1°C from 53 to 93°C. This last step allowed the melting curve of the PCR products to be determined and, consequently, their specificity. Control PCRs were similarly performed with RNA untreated by reverse transcriptase to confirm the absence of contaminating DNA in the RNA preparations, and total DNA was used as a positive control. Relative quantification of gene expression data was determined from threshold cycle (Tc) values for each sample. Serial dilutions of cDNA were used to plot a calibration curve, and gene expression levels were quantified by plotting Tc values on the curve. Expression levels were normalized with values obtained for the internal reference gene (16S rRNA). Once normalized, the transcript level at the first time point was arbitrarily set to 1, and transcript levels from next time points were plotted as the fold expression levels with reference to the levels of the first time point.

Protein techniques. Protein samples were obtained from cultures grown on cellophane disks on the surface of agar plates. The mycelium was collected and suspended in ice-cold sonication buffer (50 mM Tris-HCl, pH 8, 200 mM NaCl, 15 mM EDTA, Complete protease inhibitor cocktail [Roche Diagnostics]). Samples were sonicated (20-s bursts in ice) until a clear lysate (total protein fraction) was obtained, and samples were clarified by centrifugation (13,000 rpm for 3 min) in a benchtop microcentrifuge to remove unbroken cells and insoluble cell components (insoluble protein fraction). The supernatant was subjected to ultracentrifugation at 200,000 × *g* for 1 h at 4°C to sediment cell membranes. The pellet obtained is the total membrane protein fraction, and the resulting supernatant is the total soluble proteins fraction. Soluble protein concentrations were determined using the Bradford method (Bio-Rad), and protein concentration in the total membrane protein fraction was determined using a PlusOne 2-D Quant kit (Amersham Pharmacia Biotech) after solubilization of the membrane pellet in sonication buffer containing 50 mM 3-[(3-cholamidopropyl)-dimethylammonio]-1-propanesulfonate. Sodium dodecyl sulfate-polyacrylamide gel electrophoresis was performed as previously described (33), loading 5 μg protein per lane, and proteins were transferred to Hybond P (Amersham Pharmacia Biotech) using a Bio-Rad semidry transfer unit. Immunological detection was performed using an ECL Advance Western blotting detection kit (Amersham Pharmacia Biotech). His-tagged CrgA was detected by using Penta-His peroxidase conjugate (QIAGEN), and FtsZ was detected by using a polyclonal anti-FtsZ antibody as described elsewhere (34). The relative abundance of bands was estimated using ImageJ 1.32J (http://rsb.info.nih.gov/).

Fluorescence and immunofluorescence microscopy. Immunofluorescence microscopy was performed as described previously (34). Strains under study were grown in the acute angle of a coverslip inserted in the agar medium (NE or MS, adding 2.5 μg/ml thiostrepton if *ptipA* was to be induced). Cells were fixed using formaldehyde-glutaraldehyde, washed twice with phosphate-buffered saline (PBS), and left to dry. After rehydration in PBS for 5 min, coverslips were treated with 0.25% Triton X-100 in PBS (vol/vol) for 5 min. This treatment allows partial permeabilization of cell membranes and allows exposure of transmembrane proteins. The Triton solution was removed by three washes with PBS, and 5% bovine serum albumin–PBS (wt/vol) was added for 1 h, at room temperature, followed by three PBS washes. A 1/20 dilution of Penta-His AlexaFluor conjugate antibody (QIAGEN) in 1% bovine serum albumin–PBS was added to the coverslips and incubated overnight at 4°C. The samples were then washed 10 times with PBS and processed using Slow Fade antifade solutions (Molecular Probes) and visualized in a Nikon Eclipse E600 epifluorescence microscope. For enhanced green fluorescent protein (eGFP) visualization, the samples were processed as reported elsewhere (12). Images were acquired using a RS Photometrics digital camera and processed using Adobe Photoshop 6.0.

RESULTS

Maximal transcription of *crgA* precedes aerial development on glucose-containing media. To examine growth phase-dependent transcription of *crgA*, an integrative plasmid, pRIR1,

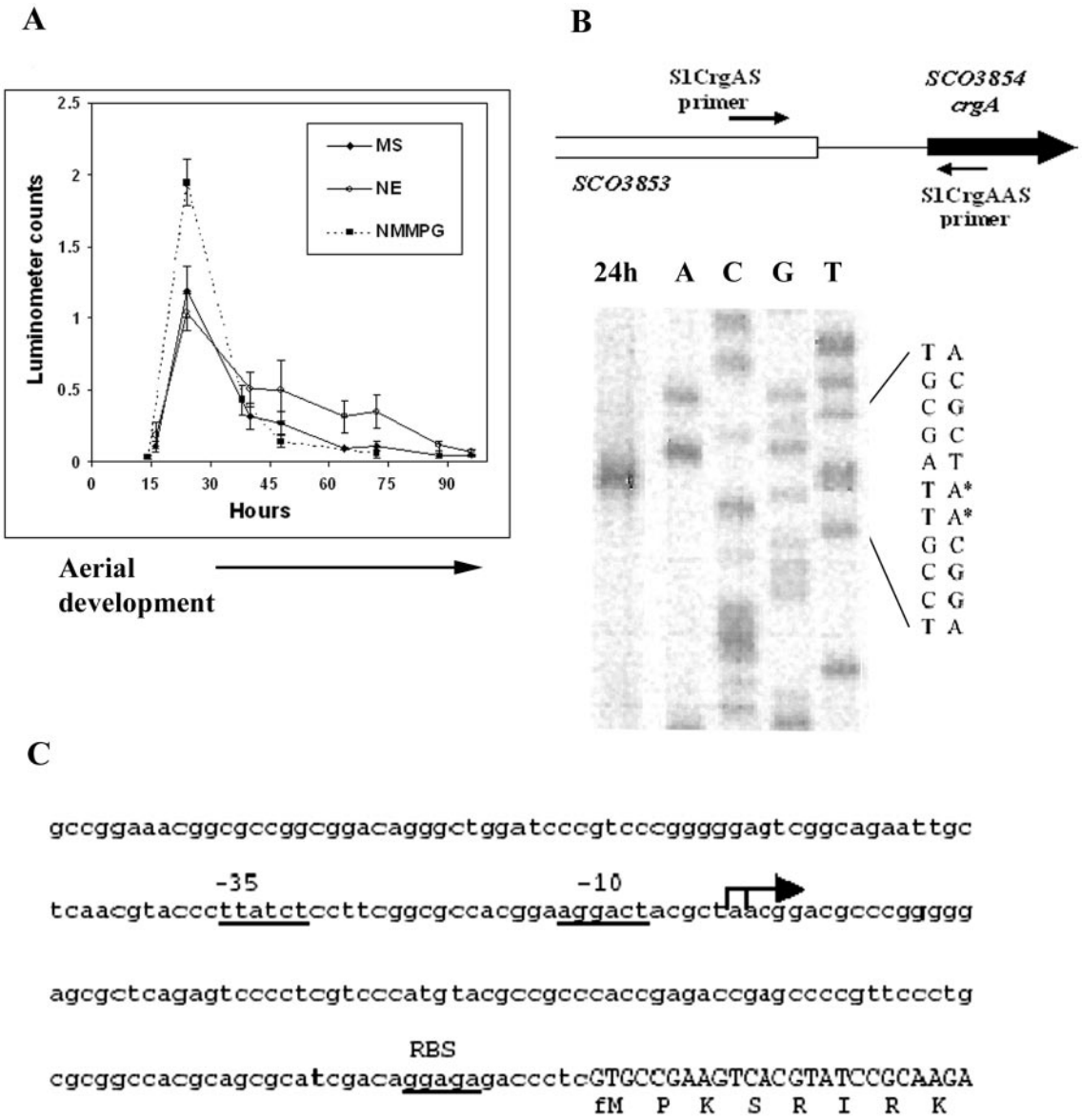

FIG. 1. Transcription of *crgA*. (A) The activity of the *crgA* promoter fused to a *luxAB* reporter cassette was determined during growth of M145/pRIR1 on solid medium and correlated with the approximate onset of morphological development as determined by visual inspection of cultures. (B) Schematic representation of primer binding sites used to generate the S1 assay probe. (C) *crgA* transcript S1 protection assay: total RNA was extracted from 24-h cultures grown on NMMP-glucose. (D) Partial sequence of *crgA*, indicating the positions of the predicted −10 and −35 motifs.

containing the promoter region fused to the *Vibrio harveyi luxAB* operon (engineered to replace TTA codons) was introduced into *S. coelicolor* M145. The activity of the promoter was determined during growth on various solid media. In each case, expression was observed to peak at approximately 24 h postinoculation and decline during subsequent morphological development (Fig. 1A). The highest levels of expression were observed during growth on glucose-containing media, for example, NMMP-glucose, on which the *crgA* mutant is phenotypically distinct. The kinetics of *crgA* transcription on this growth medium were further investigated using real-time PCR (results not shown), confirming the luciferase data. When pRIR1 was introduced into the *crgA* mutant DC3854, no significant differences could be detected between the luminescence patterns of the mutant or wild type containing this plasmid (results not shown). Consequently, there is no evidence to suggest autoregulation of *crgA* expression. The *crgA* promoter was mapped using an S1 nuclease protection assay. A probe was designed to cover the entire intergenic region between *SCO3854* and *SCO3853* (Fig. 1B). One single transcript was detected, indicating a single start site (Fig. 1C). At appropriate distances from the transcriptional start site, sequences resembling typical −10 and −35 motifs were found (Fig. 1D).

CrgA is an integral membrane protein. The abundance and subcellular localization of CrgA were analyzed by expressing a C-terminal His-tagged version of the protein. An integrative

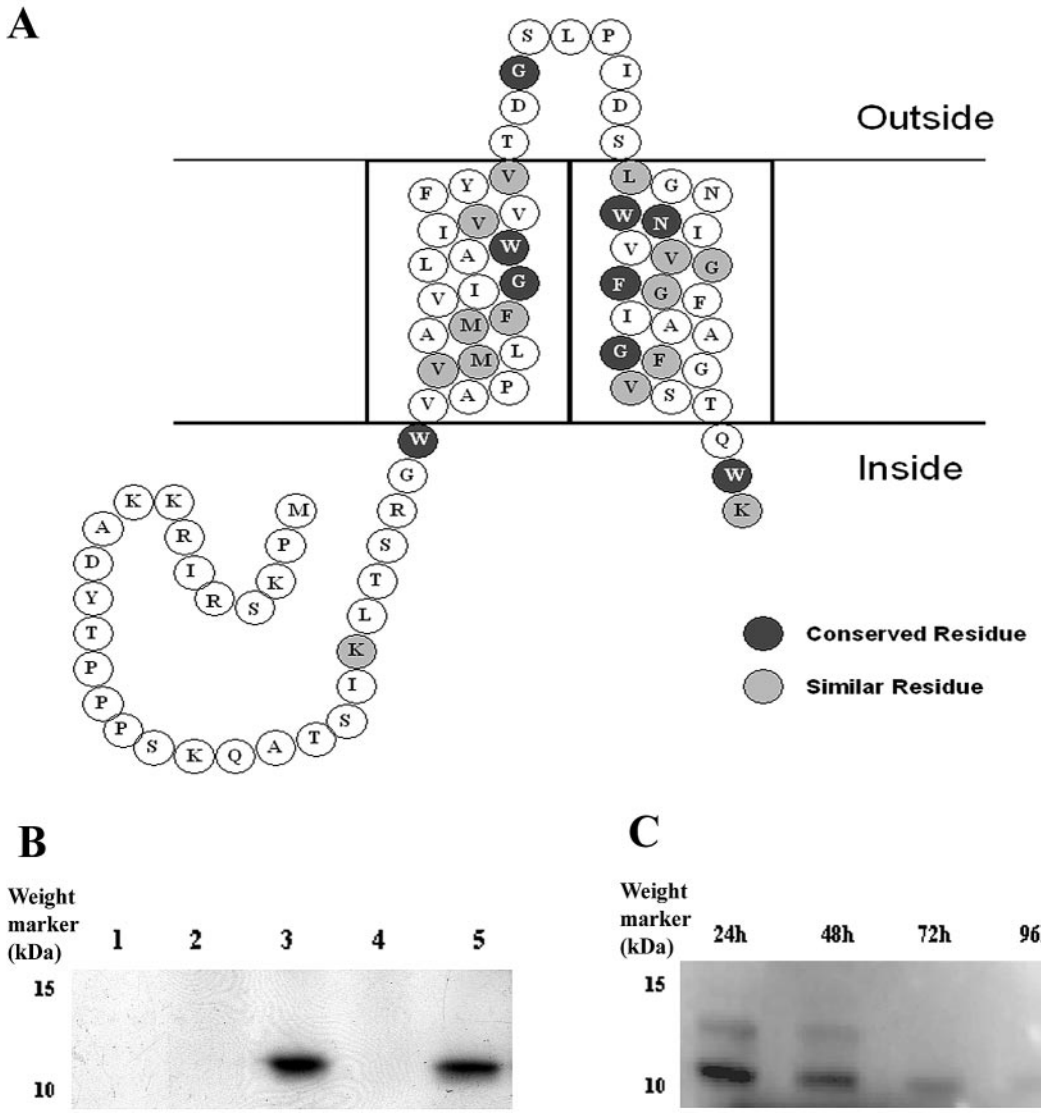

FIG. 2. Topology and membrane localization of CrgA. (A) The CrgA sequence of various actinomycetes was analyzed using topology prediction and alignment software. The two consistently predicted transmembrane regions are the most highly conserved regions of the protein, with the extramembrane regions displaying only isolated conserved residues. The sequence of *S. coelicolor* CrgA is displayed: amino acids of conserved identity are denoted by white text in dark background circles, and residues with similar properties are shown as black text in shaded circles. Swiss-Prot database accession numbers (in parentheses) and percent amino acid identities with *S. coelicolor* CrgA (Q9XA10) are as follows: *S. avermitilis* (Q93JL8), 94%; *Corynebacterium efficiens* (Q8FUI7), 31%; *C. glutamicum* (Q8NU99), 33%; *Mycobacterium leprae* (Q9CDE7), 31%; *M. tuberculosis* (P71581), 33%; *Bifidobacterium longum* (Q8G6P5), 32%; *Tropheryma whipplei* (P59486) 40%. (B) Western blot showing subcellular localization of CrgA:His_6 in *Streptomyces coelicolor*. Lanes 1 and 2, *S. coelicolor* M145 total protein and membrane protein fractions, respectively; lanes 3, 4, and 5, *S. coelicolor* DC3854/pRWHis2 total protein, soluble protein, and membrane protein fractions, respectively. Protein samples were prepared after 24 h of growth on NMMP-glucose medium. Five micrograms of total protein was loaded on each lane. (C) Detection of CrgA:His_6 in protein samples prepared from *S. coelicolor* DC3854/pRWHis2 grown on NMMP-glucose for the indicated times. Similar amounts of total protein (5 μg) were loaded on each lane.

plasmid, pRWHis2, encoding this translational fusion under control of the native *crgA* promoter was introduced into the *crgA* mutant DC3854. The fusion protein restored the timing of reproductive growth of the mutant to that of the wild type, indicating complementation and consequently no effect of the His tag on protein function (results not shown). To explore localization of the protein, cell extracts were prepared from the recombinant strain grown for 24 h. Fractions consisting of total cellular protein, soluble cytoplasmic protein, and membrane protein were prepared and analyzed by Western blotting. His-tagged CrgA could be detected only in the total and membrane protein fractions and in both as a single species (Fig. 2B). By comparison with the predicted size of the protein, no gross modifications of the fusion protein were apparent, although changes due to limited loss of N-terminal amino acids or small covalent modifications would not have been detected. To follow a time course of CrgA-His_6 abundance, total protein extracts were prepared from mycelia harvested at different times

during a growth cycle. Western blot analysis indicated the highest abundance of the protein at 24 h, with levels decreasing thereafter (Fig. 2C), consistent with the observed abundance of *crgA* transcript.

The experimental evidence is consistent with bioinformatic predictions (HMMTOP [38], TMHMM [23], and TopPred2 [39]) that CrgA is an integral membrane protein. Indeed, a high proportion, exactly half, of the 84-residue protein is predicted to be localized to the membrane, with a cytoplasmic N-terminal portion of 30 amino acids and two transmembrane regions of 21 amino acids in length and with an intervening external loop composed of 9 amino acids (Fig. 2A). The cytoplasmic C terminus is predicted to be composed of only three amino acids. Alignment of the *S. coelicolor* CrgA sequence with that of other actinomycetes (*Streptomyces avermitilis*, *Corynebacterium efficiens*, *Corynebacterium glutamicum*, *Mycobacterium leprae*, *Mycobacterium tuberculosis*, *Bifidobacterium longum*, and *Tropheryma whipplei*) using ClustalW (37) revealed a low level of sequence conservation, with only nine residues with conserved identity. Conspicuously, these are all predicted to be in the membrane or within three amino acids of the ends of the two transmembrane regions (Fig. 2A). Widening these sequence alignments to consider similar residues revealed 14 similar amino acids, again predominantly localized within the transmembrane regions. On the inside of the membrane, there is a conserved tryptophan residue on both the entry-to-transmembrane region 1 (TM1) (Trp 30) and the exit of TM2 (Trp 83). These bulky hydrophobic residues are frequently found at the interfacial regions of transmembrane helices and, being conserved in this protein, are likely to play a substantial role in producing the conserved topology of CrgA predicted for all members of this protein family.

CrgA localizes at discrete foci distal from growing hyphal tips. In situ localization of CrgA was investigated by visualizing the His-tagged protein in hyphae of DC3854 containing pRWHis2 grown on NE medium. In samples grown for 24 h, with the gene expressed from it native promoter, a nonuniform distribution of the protein was observed, with localization to discrete foci along branched substrate hyphae. Similar foci are localized away from the growing tips of unbranched hyphae that are possible immature aerial hyphae (Fig. 3B). These foci could not be detected in older samples. Ectopic expression of native CrgA causes a Whi phenotype, apparently inhibiting the formation of sporulation septa (6). A copy of the His-tagged gene fusion, under control of the thiostrepton-inducible promoter *ptipA*, was introduced into wild-type *S. coelicolor* M145. Overexpression of the tagged protein was also observed to cause a Whi phenotype on all media tested (results not shown). The localization of the overexpressed protein was determined by fluorescence microscopy. In comparison to localization of the protein expressed under its native promoter, more abundant and brighter foci were observed in 24-h (Fig. 3C and D) and 48-h samples. Moreover, these foci were distributed in all parts of the mycelium, including in the growing apical cells of unbranched aerial hyphae. Similar foci were observed when an overexpressed C-terminal fusion of CrgA with eGFP was also analyzed (Fig. 3F and G).

CrgA expression influences the dynamics of the FtsZ protein. Precocious development of a *crgA* mutant on glucose-containing medium is characterized by the formation of abundant hyphae that have undergone regular extensive multiple septation (6). We examined the initial stages of septation by introducing an FtsZ-eGFP translational fusion into both the mutant and wild type. In the latter, hyphae containing FtsZ rings were scarce at all time points examined (Fig. 4A), reflecting the poor ability of the wild-type strain to sporulate on glucose-containing growth medium. In contrast, in the *crgA* mutant, hyphae undergoing the initial stages of septation in which the assembly of FtsZ rings was evident were relatively plentiful (Fig. 4B), typically with up to three- to fourfold greater abundance (at 24 h) compared to the largest number observed in the wild type at 48 h postinoculation. In addition, the extent of the zone of each hypha in which FtsZ rings were formed was typically between 30 and 50% longer in the mutant. On mannitol-containing sporulation medium, there was no significant difference observed in the abundance of septating hyphae present in the wild type and mutant, but again the extent of the FtsZ ring zone of individual hyphae was up to 50% greater in the *crgA* mutant (results not shown). The increase in abundance of FtsZ rings in the mutant, particularly when grown on glucose-containing medium, could reflect increased expression of this cell division protein in the *crgA* mutant. Indeed, evidence from Western analysis indicated a significant difference in the profile of FtsZ expression in the mutant compared to the wild type (Fig. 4C, panels I and II). Precocious development of the mutant was reflected in somewhat elevated expression at 24 h followed by a sharp decrease in FtsZ abundance thereafter; this decline was only evident after 72 h of growth of the wild type. For both strains the decline correlated with progression to equivalent stages of morphological development when the cultures were undergoing evident sporulation (Fig. 4C, panel III).

The dynamics of FtsZ was also investigated in hyphae grown on mannitol-containing sporulation medium when CrgA was overexpressed, revealing either very diffuse fluorescence, consistent with an absence of polymerization and localization of FtsZ-eGFP, or hyphae in which the initial stages of ring formation were evident (Fig. 5B and C). In the latter, the distribution was not in regular-spaced rings but in the form of spirals with occasional irregular-spaced rings. During a 96-h growth cycle (sufficient for spore maturation in the wild type), hyphae containing regular-spaced rings were very infrequent in the strain in which CrgA was overexpressed and only detected after 72 h of growth. Prolonged incubation (up to 6 days) of the overexpression strain resulted in more abundant growth of hyphae in which regular Z-ring formation and subsequent sporulation were observed, although it is unlikely that thiostrepton induction of *crgA* was effective during growth of these cells. Western analysis of protein extracts prepared from a time course revealed a peak abundance of FtsZ in the wild type at 48 h, preceding sporulation (Fig. 5D, panel I). However, at corresponding time points in the strain overexpressing CrgA, far less FtsZ was detected (Fig. 5D, panel II). A putative proteolytic product of FtsZ was observed in these samples. To investigate if the observed low level of protein was a consequence of reduced transcription, the relative amounts of *ftsZ* transcript in the wild type and CrgA overexpression strains were compared. In contrast to the relative amounts of FtsZ protein in the two strains, the quantity of transcript in the CrgA overexpression strain was equivalent to that in the wild

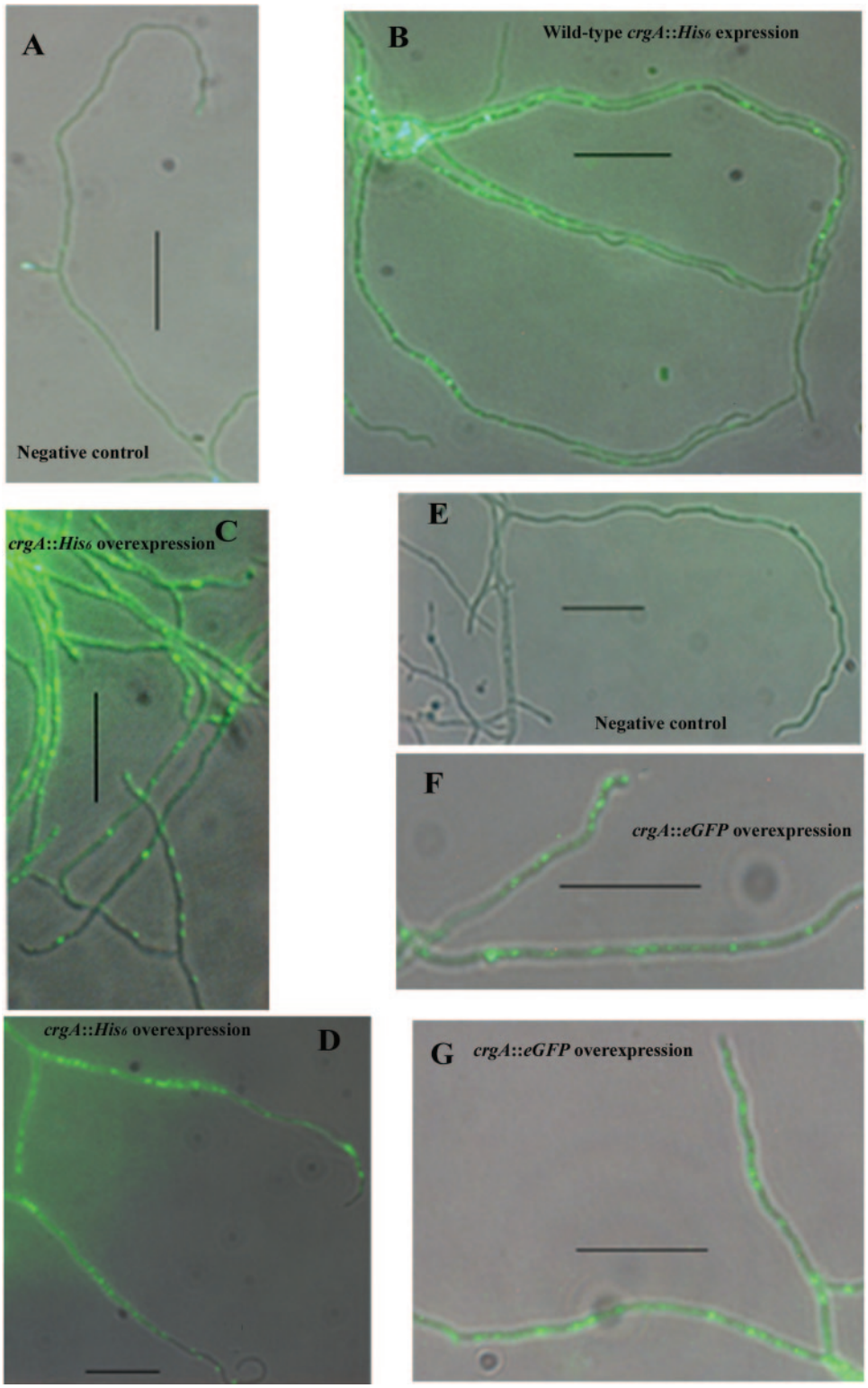

FIG. 3. In situ localization of CrgA. The in situ localization of CrgA was determined using either immunofluorescent detection of CrgA:His_6 or direct fluorescent visualization of CrgA:eGFP. Fluorescent fields that were imposed on the corresponding phase-contrast image are displayed. (A) M145/pIJ8600 (negative control); (B) *S. coelicolor* DC3854/pRWHis2 (*crgA*:[His_6] expressed from its native promoter); both strains were grown for 24 h on NE medium. (C and D) *S. coelicolor* M145/pRWHis1 (*crgA:*[*His*]$_6$ overexpressed from the *tipA* promoter); (E) *S. coelicolor* M145/pIJ8660 (negative control); (F and G) *S. coelicolor* M145/pRME43 (*crgA:eGFP* overexpressed from the *tipA* promoter). Samples shown in panels C and F were grown for 24 h on NE supplemented with 2.5 μg/ml thiostrepton; those shown in panels D, E, and G were grown for 24 h on MS supplemented with 2.5 μg/ml thiostrepton. Black arrows indicate hyphal tips. Bar, 10 μm.

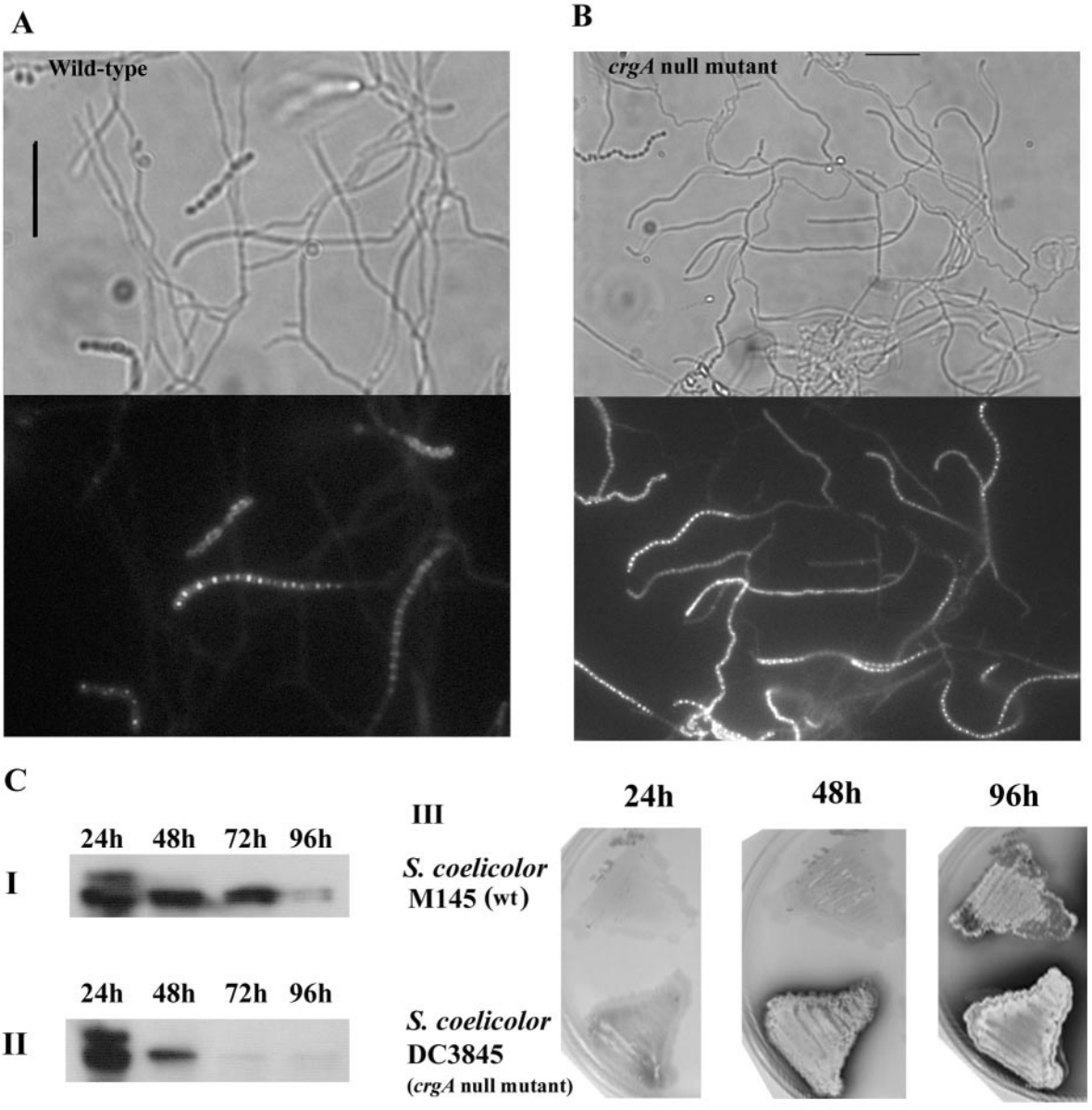

FIG. 4. Increased early Z-ring formation in a *crgA* mutant. (A and B) Visualization of Z rings in sporogenic aerial hyphae of strain M145/pKF41, 48 h postinoculation (A) and of strain DC3854/pKF41, 24 h postinoculation, grown on NE medium (B). The topmost panel of each shows the phase-contrast image, and beneath it is the corresponding fluorescence (eGFP) micrograph. Bar, 10 μm. (C) Immunoblot showing FtsZ abundance in cells grown on NE medium for the indicated times: I, strain M145; II, strain DC3854 (5 μg total protein was loaded on each lane); III, macroscopic images of both strains grown on NE medium for the indicated times.

type at all time points (Fig. 5E), consistent with no disturbance to the temporal upregulation that immediately precedes sporulation in the wild type. In the CrgA overexpression strain, both the inability to form productive rings and low abundance of FtsZ correlated with the failure of aerial hyphae to undergo evident sporulation during a normal growth cycle (Fig. 5D, panel III).

DISCUSSION

Compared to cytokinesis at the mid-cell of a unicellular bacterium, the conversion of a long syncytial hyphal cell into a chain of unigenomic prespore compartments places particular demands on how cell division is orchestrated during sporogenesis in *Streptomyces*. Indeed, our knowledge of how multiple, regular-spaced septa are formed and how this is coordinated with chromosome replication and segregation is limited. Developmental upregulation of *ftsZ* transcription occurs in sporogenic hyphae, dependent on several *whi* genes that encode early-stage sporulation regulators (10, 12). The regular placement of multiple FtsZ rings is preceded by a protracted phase during which spiral-shaped FtsZ filaments are formed along the length of an aerial hyphal cell (12). Remodelling of these filaments is believed to generate an array of regular-spaced Z

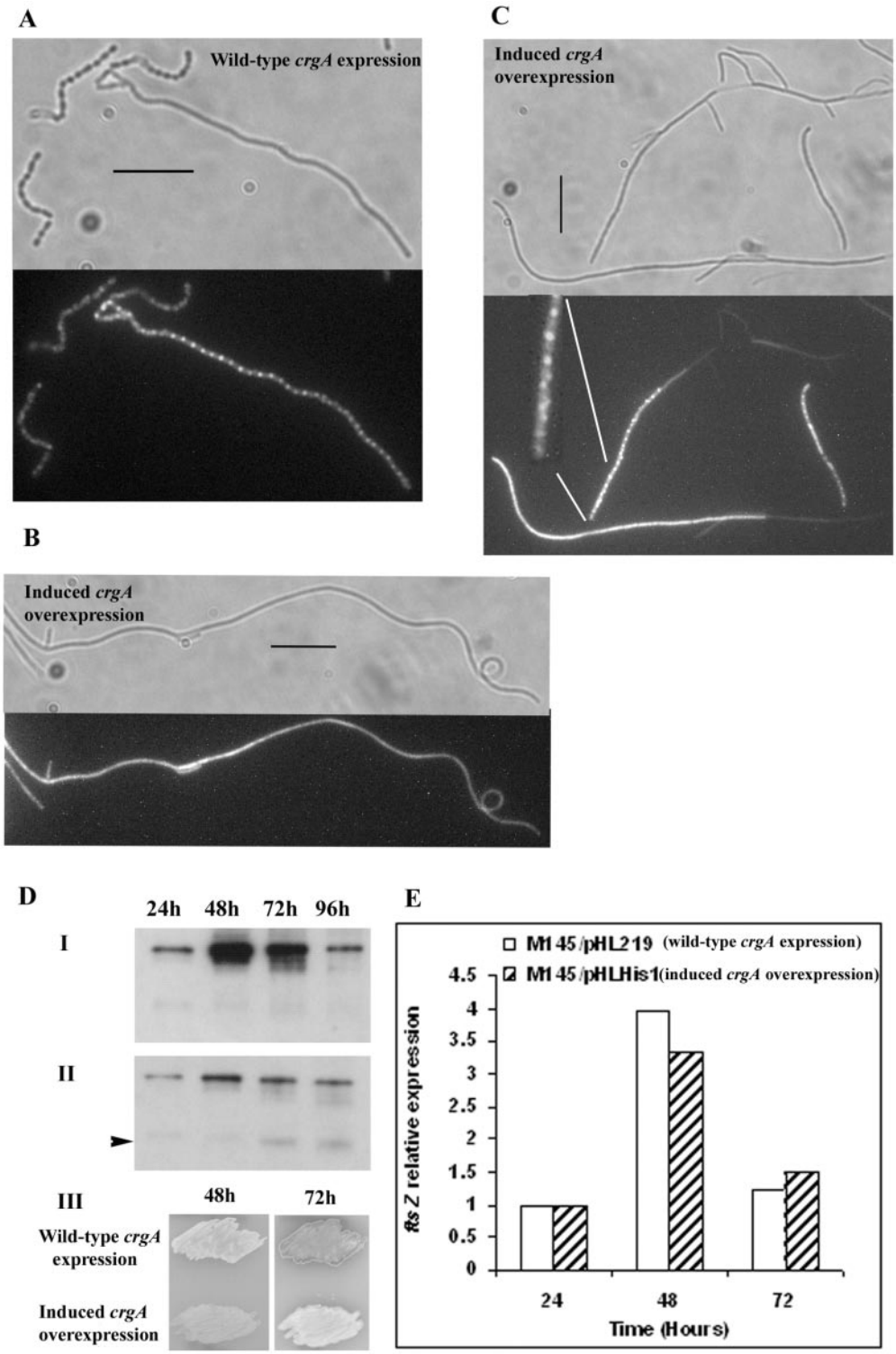

FIG. 5. Effect of CrgA overexpression on the dynamics of FtsZ. (A to C) Visualization of typical examples of sporogenic aerial hyphae of strain M145/pKF41/pHL219 containing Z rings (A), and aerial hyphae of strain M145/pKF41/pHLHis1 containing nonpolymerized FtsZ or FtsZ spirals (B and C). Hyphae were prepared after 48 h of incubation on MS medium containing thiostrepton (2.5 μg/ml). The topmost panel of each shows the phase-contrast image, and beneath it is the corresponding fluorescence (eGFP) micrograph. The inset of panel B is a threefold magnification of a region of a hyphae containing FtsZ spirals. Bar, 10 μm. (D) Immunoblots comparing FtsZ abundance in cells grown on MS medium containing 2.5 μg/ml thiostrepton for the indicated times: I, strain M145/pKF41/pHL219; II, strain M145/pKF41/pHLHis1 (5 μg total protein loaded per lane) (the arrow in panel II points to a putative FtsZ degradation product); III, macroscopic images of both strains grown on MS medium for the indicated times. (E) Comparison of the relative abundance of the *ftsZ* transcript at the indicated time points in both strains grown on MS medium containing 2.5 μg/ml thiostrepton as determined by real-time PCR.

rings, formation of which immediately precedes cytokinesis. The identity of factors that guide regular placement of Z rings is unclear. Some irregularly placed septa are observed in mutants defective in chromosome partitioning (22), suggesting some influence by this process.

In addition to the orchestration of Z-ring placement in sporogenic cells, the early events of cytokinesis must be coordinated with growth arrest of an aerial hypha and limited to apical syncytial cells. Genetic and cytological evidence indicates that CrgA has a critical function in coordinating this aspect of development, particularly during growth on glucose-containing medium. A *crgA* mutant produces a greater abundance of hyphae in which Z-ring formation and subsequent regular septation occurs, and the length of the zones of these hyphae in which cytokinesis occurs is significantly greater than in the wild type. The latter observation may be a consequence of delayed growth arrest of aerial hyphae in the mutant so that apical sporogenic cells are longer. Expression of CrgA in the wild type is primarily regulated at the level of transcription, to peak immediately before the appearance of aerial hyphae. The translated integral membrane protein then localizes to discrete foci away from the emerging hyphal tips. Evidence that CrgA inhibits Z-ring formation comes from ectopic overexpression, leading to CrgA foci distributed throughout the length of the aerial hyphae. In this case developmental upregulation of *ftsZ* in sporogenic cells was evident, but the protein was not assembled into regularly placed rings. Evidently, in these cells CrgA affects either correct remodeling of spirals or the stability of FtsZ polymers; the failure to form rings underlies the inability for these cells to undergo sporulation septation.

CrgA expression not only influences the dynamics of Z-ring formation, but also has a dramatic effect on the timing of FtsZ expression and its turnover. After 24 h growth, in the absence of CrgA, the organism undergoes precocious development and concomitant transient upregulation of FtsZ expression. The level of FtsZ protein in the mutant subsequently declines rapidly; this level of turnover is not seen for another 48 h in the wild type. Protein turnover after transcriptional upregulation of *ftsZ* has a precedent in another differentiating bacterium, *Caulobacter crescentus* (20, 29). In this organism, transcription of *ftsZ* is upregulated to allow the initiation of cell division in stalked cells. Immediately afterwards, FtsZ undergoes rapid proteolysis, especially in progeny motile swarmer cells that are consequently unable to initiate cytokinesis until after an obligatory gap period. Developmentally programmed proteolysis of FtsZ in spore-forming cells of *S. coelicolor* is likely to be important in establishing dormancy, as the spores mature prior to their dispersal.

In contrast to precocious upregulation of FtsZ expression in the absence of CrgA, overexpression of the latter reduces the levels of FtsZ protein in sporogenic hyphae. This is not a consequence of a failure to upregulate transcription. Rather, the observed reduction in levels of FtsZ is presumably a consequence of higher turnover of the protein. This turnover may result from the failure to remodel FtsZ spiral filaments into productive Z rings, stabilized by association with other cell division proteins (the divisome).

How does CrgA function? A precedent for a membrane-associated inhibitor of Z-ring formation is EzrA of *Bacillus subtilis* (14, 24). This protein can interact directly with FtsZ, preventing its polymerization. However, our evidence suggests a different mode of action for CrgA. Firstly, FtsZ polymer spirals, but not productive Z rings, are formed in hyphae in which CrgA is overexpressed. Secondly, EzrA is distributed throughout the plasma membrane of dividing cells, but it also concentrates at the cytokinetic ring in an FtsZ-dependent manner (14). This localization pattern is interpreted as implying that EzrA prevents Z-ring assembly anywhere along the inner surface of the membrane. A Z ring is formed at the mid-cell due to the activity of an as-yet-unidentified temporally regulated positive factor that can overcome the inhibitory activity of EzrA. The latter can then interact with FtsZ polymers but not promote disassembly. In contrast, CrgA is localized to foci in hyphal cells in which Z rings that precede sporulation septa are absent. Lastly, EzrA and CrgA have quite different topologies. The former has a single 26-residue membrane-spanning domain. Although deletion of this anchor interferes with the protein's function in vivo, the remaining 236-residue cytoplasmic domain is sufficient to inhibit FtsZ assembly in vitro (14). In contrast, the two transmembrane domains of CrgA comprise half of the protein, and the only significant cytoplasmic portion of the protein is a 30-residue nonconserved N-terminal domain. Overexpression of this cytoplasmic domain, after deletion of both transmembrane domains, has no effect on sporulation (results not shown). Identity between full-length *S. coelicolor* CrgA and nonstreptomycete orthologs in other actinobacteria is between 28 and 40%. This contrasts with the >65% identity shared between FtsZ proteins from the same species. The conserved residues of CrgA are all immediately at the boundaries of or within the transmembrane domains. Several of these residues are likely to promote intimate interhelical interactions between TM1 and TM2, supporting a hairpin-like topology of the protein. The internal half of TM1 is rich in large branched chain residues at appropriate depths to enable their interaction with glycine residues (including the conserved Gly 76 and widely found Gly 71) located in the internal half of TM2. Conversely, at the middle of the membrane, there is a conserved glycine residue (Gly 42) on TM1 that is predicted to interact with either the conserved Phe 70 or Val 68, both at the appropriate membrane depth, on TM2. Towards the outer halves of the two transmembrane domains there is decidedly less scope for close helix packing. Indeed, the successive conserved bulky Trp 64 and polar Asn 65 residues of TM2, opposite a bulky and hydrophobic portion of TM1, suggest a possible role for this region in specific interactions with other proteins. Importantly, the topology predictions and absence of any conservation of the cytoplasmic domain both suggest that, in contrast to EzrA, CrgA itself does not directly interact with cytoplasmic FtsZ. Instead, interactions, possibly with other membrane-associated protein components of the divisome, may be critical in preventing remodelling of FtsZ spirals. In *E. coli*, both ZipA and FtsA are implicated in tethering Z rings to the membrane via their respective transmembrane domains (27, 28). The fully sequenced actinomycetes lack orthologs of these proteins. FtsZ from *M. tuberculosis* can interact with FtsW (Rv2154c), an integral membrane protein, through sequences in these proteins that appear to be unique to this genus (5). The identity of the anchor in *Streptomyces* is unclear: there are four *ftsW*/*rodA*-like genes in *S. coelicolor*, but the corresponding proteins do not possess a similar C-terminal tail

to that of the *M. tuberculosis* FtsW implicated in FtsZ interaction.

crgA is present as a single copy in all sequenced actinomycete genomes, including intracellular pathogens with severely reduced genomes such as *T. whipplei* and *M. leprae*, but not other prokaryotes. All the sequenced actinomycete genomes also lack orthologs of *minC* or *ezrA*. We propose that CrgA has an important role as an inhibitor of Z-ring formation in actinomycetes generally, coordinating growth with cytokinesis. A conservation of function is supported by the conserved location of the gene, close to *oriC* and bordering a conserved morphogenic cluster. This cluster includes genes encoding RodA (SCO3846 in *S. coelicolor*; Rv0017c in *M. tuberculosis*) and a penicillin binding protein, both of which that have been implicated in peptidoglycan synthesis during bacterial growth (7), and a signaling kinase containing PASTA (penicillin-binding protein and serine-threonine kinase associated) domains involved in the control of cell shape in *M. tuberculosis* (18, 41). Further insight into CrgA function is of particular importance in understanding cell division in pathogenic actinomycetes such as *M. tuberculosis*, against which there is an urgent need to develop new chemotherapeutics.

ACKNOWLEDGMENTS

We are grateful to Paul Herron, Department of Bioscience, University of Strathclyde, Glasgow, Scotland, for providing plasmids and Sue Fielding, University of Wales Swansea, for help with DNA sequencing. R.D.S. was supported, in part, by BBSRC grant 58/EGH18395.

REFERENCES

1. **Addinall, S. G., and B. Holland.** 2002. The tubulin ancestor, FtsZ, draughtsman, designer and driving force for bacterial cytokinesis. J. Mol. Biol. **318:** 219–236.
2. **Bierman, M., R. Logan, K. O'Brien, E. T. Seno, R. N. Rao, and B. E. Schoner.** 1992. Plasmid cloning vectors for the conjugal transfer of DNA from Escherichia coli to Streptomyces spp. Gene **116:**43–49.
3. **Bignell, D. R., J. L. Warawa, J. L. Strap, K. F. Chater, and B. K. Leskiw.** 2000. Study of the bldG locus suggests that an anti-anti-sigma factor and an anti-sigma factor may be involved in Streptomyces coelicolor antibiotic production and sporulation. Microbiology **146:**2161–2173.
4. **Chater, K. F.** 2001. Regulation of sporulation in Streptomyces coelicolor A3(2): a checkpoint multiplex? Curr. Opin. Microbiol. **4:**667–673.
5. **Datta, P., A. Dasgupta, S. Bhakta, and J. Basu.** 2002. Interaction between FtsZ and FtsW of Mycobacterium tuberculosis. J. Biol. Chem. **277:**24983–24987.
6. **Del Sol, R., A. Pitman, P. Herron, and P. Dyson.** 2003. The product of a developmental gene, *crgA*, that coordinates reproductive growth in *Streptomyces* belongs to a novel family of small actinomycete-specific proteins. J. Bacteriol. **185:**6678–6685.
7. **de Pedro, M. A., W. D. Donachie, J. V. Holtje, and H. Schwarz.** 2001. Constitutive septal murein synthesis in *Escherichia coli* with impaired activity of the morphogenetic proteins RodA and penicillin-binding protein 2. J. Bacteriol. **183:**4115–4126.
8. **Errington, J., R. A. Daniel, and D. J. Scheffers.** 2003. Cytokinesis in bacteria. Microbiol. Mol. Biol. Rev. **67:**52–65.
9. **Flardh, K.** 2003. Growth polarity and cell division in Streptomyces. Curr. Opin. Microbiol. **6:**564–571.
10. **Flardh, K., E. Leibovitz, M. J. Buttner, and K. F. Chater.** 2000. Generation of a non-sporulating strain of Streptomyces coelicolor A3(2) by the manipulation of a developmentally controlled ftsZ promoter. Mol. Microbiol. **38:** 737–749.
11. **Flett, F., V. Mersinias, and C. P. Smith.** 1997. High efficiency intergeneric conjugal transfer of plasmid DNA from Escherichia coli to methyl DNA-restricting streptomycetes. FEMS Microbiol. Lett. **155:**223–229.
12. **Grantcharova, N., U. Lustig, and K. Flardh.** 2005. Dynamics of FtsZ assembly during sporulation in *Streptomyces coelicolor* A3(2). J. Bacteriol. **187:** 3227–3237.
13. **Grantcharova, N., W. Ubhayasekera, S. L. Mowbray, J. R. McCormick, and K. Flardh.** 2003. A missense mutation in ftsZ differentially affects vegetative and developmentally controlled cell division in Streptomyces coelicolor A3(2). Mol. Microbiol. **47:**645–656.
14. **Haeusser, D. P., R. L. Schwartz, A. M. Smith, M. E. Oates, and P. A. Levin.** 2004. EzrA prevents aberrant cell division by modulating assembly of the cytoskeletal protein FtsZ. Mol. Microbiol. **52:**801–814.
15. **Harry, E. J.** 2001. Bacterial cell division: regulating Z-ring formation. Mol. Microbiol. **40:**795–803.
16. **Hopwood, D. A., M. J. Bibb, K. F. Chater, T. Kieser, C. J. Bruton, H. M. Kieser, D. P. Lydiate, C. P. Smith, J. M. Ward, and H. Schrempf.** 1985. Genetic manipulation of *Streptomyces*: a laboratory manual. John Innes Foundation, Norwich, United Kingdom.
17. **Hu, Z., A. Mukherjee, S. Pichoff, and J. Lutkenhaus.** 1999. The MinC component of the division site selection system in Escherichia coli interacts with FtsZ to prevent polymerization. Proc. Natl. Acad. Sci. USA **96:**14819–14824.
18. **Kang, C. M., D. W. Abbott, S. T. Park, C. C. Dascher, L. C. Cantley, and R. N. Husson.** 2005. The Mycobacterium tuberculosis serine/threonine kinases PknA and PknB: substrate identification and regulation of cell shape. Genes Dev. **19:**1692–1704.
19. **Kelemen, G. H., and M. J. Buttner.** 1998. Initiation of aerial mycelium formation in *Streptomyces*. Curr. Opin. Microbiol. **1:**656–662.
20. **Kelly, A. J., M. J. Sackett, N. Din, E. Quardokus, and Y. V. Brun.** 1998. Cell cycle-dependent transcriptional and proteolytic regulation of FtsZ in Caulobacter. Genes Dev. **12:**880–893.
21. **Kieser, T., M. J. Bibb, M. J. Buttner, K. F. Chater, and D. A. Hopwood.** 2000. Practical *Streptomyces* genetics. The John Innes Foundation, Norwich, United Kingdom.
22. **Kim, H. J., M. J. Calcutt, F. J. Schmidt, and K. F. Chater.** 2000. Partitioning of the linear chromosome during sporulation of *Streptomyces coelicolor* A3(2) involves an *oriC*-linked *parAB* locus. J. Bacteriol. **182:**1313–1320.
23. **Krogh, A., B. Larsson, G. von Heijne, and E. L. Sonnhammer.** 2001. Predicting transmembrane protein topology with a hidden Markov model: application to complete genomes. J. Mol. Biol. **305:**567–580.
24. **Levin, P. A., I. G. Kurtser, and A. D. Grossman.** 1999. Identification and characterization of a negative regulator of FtsZ ring formation in Bacillus subtilis. Proc. Natl. Acad. Sci. USA **96:**9642–9647.
25. **Lutkenhaus, J., and S. G. Addinall.** 1997. Bacterial cell division and the Z ring. Annu. Rev. Biochem. **66:**93–116.
26. **Margolin, W.** 2001. Spatial regulation of cytokinesis in bacteria. Curr. Opin. Microbiol. **4:**647–652.
27. **Pichoff, S., and J. Lutkenhaus.** 2005. Tethering the Z ring to the membrane through a conserved membrane targeting sequence in FtsA. Mol. Microbiol. **55:**1722–1734.
28. **Pichoff, S., and J. Lutkenhaus.** 2002. Unique and overlapping roles for ZipA and FtsA in septal ring assembly in Escherichia coli. EMBO J. **21:**685–693.
29. **Quardokus, E., N. Din, and Y. V. Brun.** 1996. Cell cycle regulation and cell type-specific localization of the FtsZ division initiation protein in Caulobacter. Proc. Natl. Acad. Sci. USA **93:**6314–6319.
30. **RayChaudhuri, D.** 1999. ZipA is a MAP-tau homolog and is essential for structural integrity of the cytokinetic FtsZ ring during bacterial cell division. EMBO J. **18:**2372–2383.
31. **Romberg, L., and P. A. Levin.** 2003. Assembly dynamics of the bacterial cell division protein FTSZ: poised at the edge of stability. Annu. Rev. Microbiol. **57:**125–154.
32. **Ryding, N. J., G. H. Kelemen, C. A. Whatling, K. Flardh, M. J. Buttner, and K. F. Chater.** 1998. A developmentally regulated gene encoding a repressor-like protein is essential for sporulation in Streptomyces coelicolor A3(2). Mol. Microbiol. **29:**343–357.
33. **Sambrook, J., E. F. Fritsch, and T. Maniatis.** 1989. Molecular cloning: a laboratory manual, 2nd ed. Cold Spring Harbor Laboratory Press, Cold Spring Harbor, N.Y.
34. **Schwedock, J., J. R. McCormick, E. R. Angert, J. R. Nodwell, and R. Losick.** 1997. Assembly of the cell division protein FtsZ into ladder-like structures in the aerial hyphae of Streptomyces coelicolor. Mol. Microbiol. **25:**847–858.
35. **Stricker, J., P. Maddox, E. D. Salmon, and H. P. Erickson.** 2002. Rapid assembly dynamics of the Escherichia coli FtsZ-ring demonstrated by fluorescence recovery after photobleaching. Proc. Natl. Acad. Sci. USA **99:**3171–3175.
36. **Sun, J., G. H. Kelemen, J. M. Fernandez-Abalos, and M. J. Bibb.** 1999. Green fluorescent protein as a reporter for spatial and temporal gene expression in Streptomyces coelicolor A3(2). Microbiology **145:**2221–2227.
37. **Thompson, J. D., D. G. Higgins, and T. J. Gibson.** 1994. CLUSTAL W: improving the sensitivity of progressive multiple sequence alignment through sequence weighting, position-specific gap penalties and weight matrix choice. Nucleic Acids Res. **22:**4673–4680.
38. **Tusnady, G. E., and I. Simon.** 1998. Principles governing amino acid composition of integral membrane proteins: application to topology prediction. J. Mol. Biol. **283:**489–506.
39. **von Heijne, G.** 1992. Membrane protein structure prediction. Hydrophobicity analysis and the positive-inside rule. J. Mol. Biol. **225:**487–494.
40. **Yanisch-Perron, C., J. Vieira, and J. Messing.** 1985. Improved M13 phage cloning vectors and host strains: nucleotide sequences of the M13mp18 and pUC19 vectors. Gene **33:**103–119.
41. **Yeats, C., R. D. Finn, and A. Bateman.** 2002. The PASTA domain: a beta-lactam-binding domain. Trends Biochem. Sci. **27:**438.